

Protein structure classification based on X-ray laser induced Coulomb explosion*

Tomas André, Ibrahim Dawod,[†] Sebastian Cardoch, Nicușor Tîmneanu, and Carl Caleman[‡]
Department of Physics and Astronomy, Uppsala University, Box 516, SE-751 20 Uppsala, Sweden.

Emiliano De Santis[§]
Department of Chemistry – BMC, Uppsala University, Box 576, SE-751 23 Uppsala, Sweden.
(Dated: October 22, 2024)

We simulated the Coulomb explosion dynamics due to the fast ionization induced by high-intensity X-rays in six proteins that share similar atomic content and shape. We followed and projected the trajectory of the fragments onto a virtual detector, providing a unique explosion footprint. After collecting 500 explosion footprints for each protein, we utilized principal component analysis and t-distributed stochastic neighbor embedding to classify these. The results show that the classification algorithms were able to separate proteins on the basis of explosion footprints from structurally similar proteins into distinct groups. The explosion footprints, therefore, provide a unique identifier for each of the proteins. We envision that method could be used concurrently with single particle coherent imaging experiments to provide additional information on shape, mass, or conformation.

I. INTRODUCTION

Radiation damage studies have been of interest since the idea of Single Particle Imaging (SPI) was first introduced [1]. SPI aims to obtain structural information from non-crystalline samples with high-intensity femtosecond duration X-ray pulses from an X-ray Free-Electron Laser (XFEL) that elastically scatter onto a detector [2]. So far, atomic resolution reconstruction of nanometer-sized systems such as single proteins has been hindered by several technical challenges [3]. One aspect of fundamental importance is the X-ray-induced damage that destroys the sample. Photons with energies commonly used for imaging experiments primarily photoionize, leaving atoms in excited electronic states that, within femtoseconds, decay radiatively and non-radiatively. Free electrons originating from these events cause additional changes to the electronic configuration through collision. In small proteins, this secondary damage is not as severe since free electrons with a mean free path greater than the particle's size escape, leaving behind charged ions [4]. The excess positive charge buildup leads to significant electrostatic forces that break the structure apart in a process known as Coulomb explosion.

Coulomb explosion imaging is a single-molecule structural determination technique of a sample stripped of its electrons, that traces the fragments by measuring the momenta of the resulting ions in coincidence [5]. XFELs provide a tool to carry out Coulomb explosion imaging since X-rays can be tuned to target specific inner shells while reaching highly-charged states via sequential single-photon absorption [6–8]. Östlin *et al.* [9] simulated X-ray-induced Coulomb explosions on lysozyme to construct time-integrated *explosion footprints* generated by projecting carbon and sulphur ions trajectories

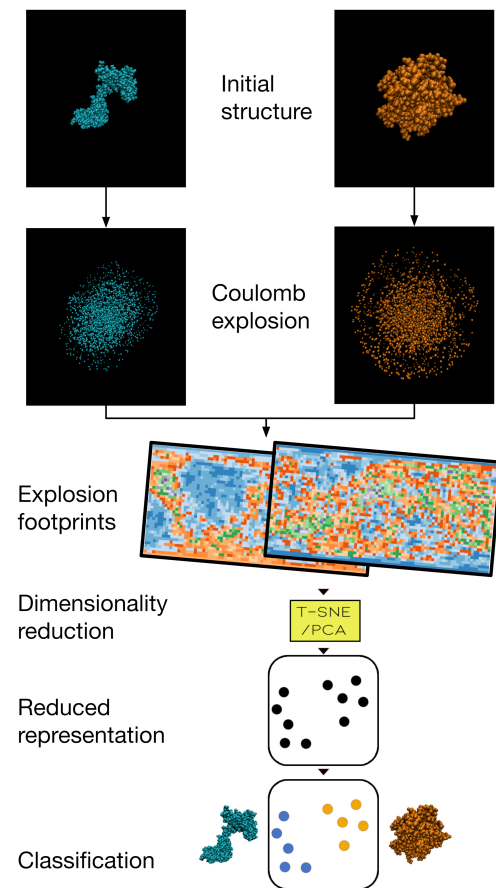


Figure 1: Conceptual overview of the process. First, the system is simulated under the exposure of an XFEL pulse using the MC/MD code, MOLDSTRUCT. Afterwards, we create the explosion footprints from the trajectories. The data are then fed through a dimensionality reduction funnel, making the high-dimensional footprints more comparable. We can then show the reduced footprints as points in a 2D space. Lastly, in this 2D space we can employ clustering to classify the data.

* ESI available at:

[†] Also at European XFEL, Holzkoppel 4, DE-22869 Schenefeld, Germany.

[‡] carl.caleman@physics.uu.se; Also at Center for Free-Electron Laser Science, Deutsches Elektronen-Synchrotron, Notkestraße 85 DE-22607 Hamburg, Germany.

[§] Also at University of Rome Tor Vergata & INFN, Rome, 00133, Italy.

onto a virtual detector and concluded these maps could be used to determine the protein’s orientation during exposure. Our present study takes this idea further by classifying explosion footprints on three pairs of proteins that share stoichiometric and conformational similarities. Unlike conventional Coulomb explosion images, the explosion footprints used in this study are constructed uniquely from ion trajectories and carry no coincidence or momentum information.

In this simulation study, we aim to answer the following question: *In an XFEL experiment, is it feasible to separate structurally similar proteins solely based on the explosion footprint?* To do this we model the interaction between the X-ray laser and single proteins using a Monte Carlo/Molecular Dynamics (MC/MD) code, similar to [10], that computes electronic occupation and ion dynamics. After tracing the ions’ trajectory, we carry out a dimensionality reduction to project explosion footprints in two dimensions to assess if sufficient structural information is preserved to uniquely separate explosion footprints from similar proteins. A schematic summarizing our work is presented in Fig. 1. We see this study as a first step to develop a technique that can capture additional complementary information during SPI experiments to aid orientation recovery algorithms such as expansion-maximization-compression needed for reconstruction [11, 12].

II. RESULTS

We begin by preparing the simulation environment, for the systems outlined in Table I. To quantify the similarity of the three selected pairs of proteins, we use the local Distance Difference Test (IDDT) [13], calculated using [14]. IDDT is a superposition-free score which evaluates local distance differences in a model compared to a reference structure. The IDDT values span from 0 to 1, where 1 corresponds to perfect structural match.

Each protein is placed in a vacuum at a fixed orientation, and after a standard equilibration procedure, we acquire snapshots of the structure at distinct time steps to perform MC/MD simulations. Model details are available in the SI. The Coulomb explosions are triggered by a temporal Gaussian-shaped X-ray pulse with a 10 fs full width at half maximum duration, 600 eV photon energy, and 5×10^6 photons/nm² fluence. We perform 500 simulations for every protein that follow the electron occupation and ion dynamics as a function of time. After 100 fs from the exposure, we project the resulting ion trajectories onto a unit sphere using the direction of the unit velocity vector. See the SI for additional details. To visualize the explosion footprints, the spherical signal is distorted into two dimensions (equiangular projection), akin to some world maps, resembling a theoretical full spatial area detector, with the x- and y-axes representing azimuthal and elevation angles, respectively. Examples of these two-dimensional footprints are shown in Fig. 2. The averages of many footprints originating from the same protein can easily be distinguished by eye. However, singular footprints exhibit high variance due to differences in the protein structure at the moment of exposure and the inherent probabilistic nature of

photon-matter interaction.

To classify the footprints on an individual basis, we make use of principal component analysis (PCA) [19] and t-distributed stochastic neighbor embedding (t-SNE) [20] to reduce the dimensionality of each explosion footprint to two dimensions. We use both techniques since they highlight different aspects of the problem. The t-SNE method produces a reduced space much more suitable for clustering algorithms, i.e. well separated clusters of similar sizes. The PCA method preserves distances, making it easier to compare systems. The clustering itself is done using k-means, a simple clustering algorithm that groups similar data points together by finding the best centers for each group and iteratively adjusting these centers until the groups are as compact and distinct as possible.

The PCA and t-SNE scatter plots of the explosion footprints in the reduced spaces are shown in Fig. 3. Both algorithms can easily separate the monomer and dimer of the same protein, depicted as dark and light green dots. The algorithms are also able to separate two of the same protein in two different conformations, with one being compact and the other stretched, shown as dark and light yellow dots. Comparing how PCA places the clusters, we note that PCA seems to regard the monomer more similar to the compact and the stretched structures, which is interesting since this is not obvious to the human eye looking at the footprints, Fig. 2. The final and most astonishing result is that t-SNE is able to separate asymmetric and symmetric structures, depicted as light and dark blue dots. These two proteins have the same amino acid sequence and their structures are almost identical. The main differences between them are their distinct FG loops. For the symmetric structure, all FG loops are well defined β -hairpins, while for the asymmetric structure one of the FG loops is collapsed towards the main protein body [21]. Despite this very subtle difference, t-SNE clearly separates the two structures, while PCA is not capable of doing so.

To evaluate the quality in the clustering we employ the adjusted random score (ARS) [22], a measure to compare the similarity of two sets of clusters, on a scale between 1 and -1. A value of 1 indicates perfect agreements between the clusters, 0 indicates similarities between clusters are random, and -1 indicates perfect disagreement. By setting one set of clusters to the correct values and the other set of clusters to the predicted values, we can use the ARS as a metric for how well the predicted clusters fit the correct clusters. By computing the ARS of the k-means predicted clusters and the true-labels, we find the PCA achieves a value of 0.97 and t-SNE a value of 1.00. This means that t-SNE are able to group individual explosion footprints together with perfect precision, at least in our study.

It should be kept in mind that these footprints are not normalized, therefore information about number of atom and by extension their approximate mass (due to a positive correlation between number atoms and atomic mass in the proteins we study) is encoded via the intensity variations. In an attempt to estimate whether the algorithms would work even if we removed the information about the number of atoms in the proteins, we normalized all the integrated intensities in the footprints to one. We note that we achieve similar ARS values

Systems	HiPIP [15]		Calmodulin [16, 17]		MS2 coat protein [18]	
PDB-name	5D8V	5D8V	1PRW	3CLN	2MS2	2MS2
Alias	Dimer	Monomer	Compact	Stretched	Sym	Asym
Atoms	2430	1215	2184	2240	3858	3858
IDDT	0.38		0.77		0.89	

Table I: Information about the three different systems we investigate, the HiPIP dimer/monomer [15], the stretched/compact calmodulin [16, 17] proteins and the symmetric and asymmetric dimers of the MS2 virus [18]. We list the names used by the PDB-database, the alias we will refer to them as and the number of atoms (hydrogen atoms included) in each protein. We also list the pairwise IDDT score [13] between the proteins in the system. For a visual representation see Fig. 2.

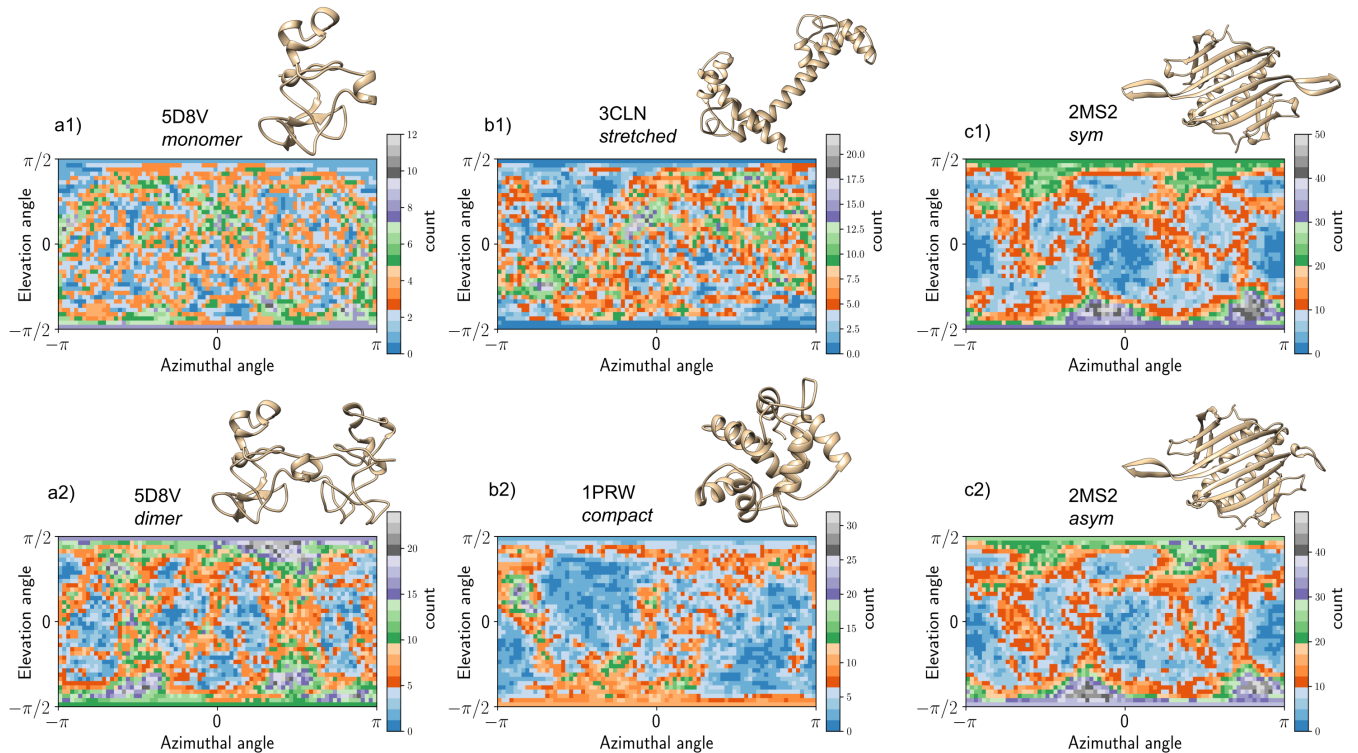


Figure 2: Visual representation of systems together with an explosion footprint from a singular explosion, labeled after the different cases studied. Three pairs of systems were selected for this study. First monomer a1) and a dimer a2) of a High-Potential Iron-sulfur Protein. The second pair was two systems with similar atom count but different structure: b1) a stretched and b2) a compact folding of a calmodulin protein. The last pair is the one we expect to be hardest to separate: c1) a symmetric and c2) asymmetric folding of the MS2 virus coat protein.

and reduced spaces using our normalized footprints (results not shown) as in Fig. 3, thus the clustering is not exclusively measuring the number of atoms, which would essentially just be counting the mass.

The results presented so far assume we know the orientation of the protein, which is typically not the case for SPI experiments done today. However, attempts to pre-orient the proteins with external electric fields exist [23], and earlier studies indicate that the orientation can be retrieved from the explosions [9]. In addition, in an SPI experiment where the diffraction image is recorded simultaneously, these can be used to find the orientation [12]. We attempt to distinguish explosion footprints using t-SNE without any knowledge about the orientation and find the only two systems that are possible to

separate are the dimer and the monomer (results not shown).

So far in our study we considered the usage of a spherical 4π -detector, which is an idealization that is not feasible using current experimental setups. By removing the outer pixels of the explosion footprints we can reduce the solid average coverage and approach something more similar to a planar detector as seen in Fig. 4a. To gauge how this impacts the clustering we calculate the ARS from clustering the reduced t-SNE spaces while incrementally trimming the edges of the image, effectively utilizing only a central portion of the detector while maintaining the original solid angle per pixel resolution. We present the dependence in Fig. 4b. We see that the clustering remains effective even for smaller planar-like detectors, with a detector area that would be feasible to cover experimentally.

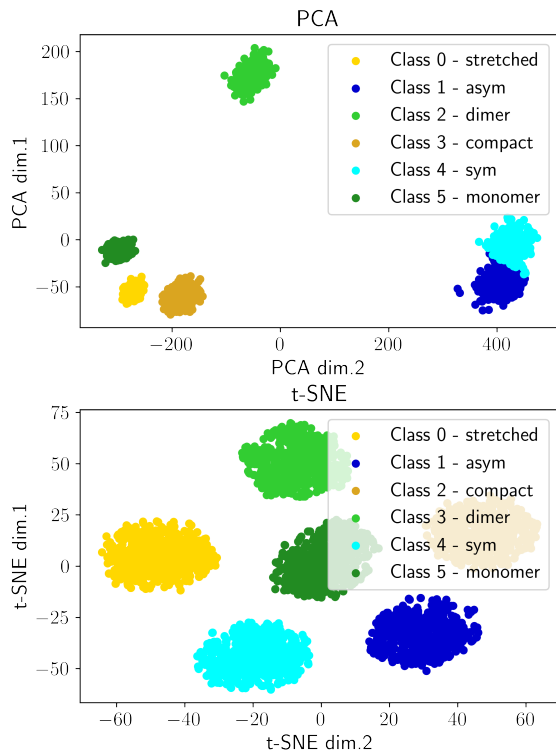


Figure 3: Scatter plots of the protein explosion footprints in the reduced space, with dimensionality reduction by PCA [19] (top) and t-SNE [20] (bottom). The clustering is evaluated with the adjusted random score, where PCA gives a score of 0.97 and t-SNE achieves the maximum score of 1.00, a perfect match. The original orientation of the proteins was kept fixed and all proteins can be classified in distinct classes. The classes are predicted by k-means and labeled to what system they mainly correspond to.

III. DISCUSSION AND CONCLUSION

We have used a Monte Carlo/Molecular Dynamics model to simulate Coulomb explosions of 6 different proteins initiated by ultrafast X-ray pulses from X-ray Free Electron Lasers. By mimicking a full-spatial detector we can extract the directions of the ions, from which we can create a unique explosion footprint. By using the explosion data from proteins with known orientation, we have been able to accurately classify all of the different proteins across all degrees of structural variations. We also demonstrated the robustness of the classification for detectors covering smaller solid angles 4b. Based on the assumption that proteins exposed to an intense X-ray pulse explode in a reproducible manner, we have investigated the possibility to use the information contained in the explosion to separate proteins based on structure. This is the first step towards finding ways to extract more detailed structural information from measuring the direction of ions ejected from

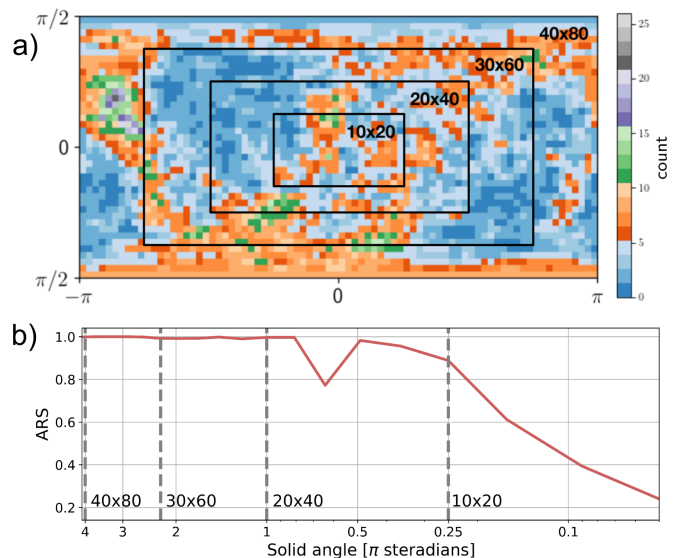


Figure 4: **a)** Explosion footprint showing different detector sizes. **b)** Adjusted random score based on the reduced t-SNE spaces compared between different sizes of detectors. Each pixel covers an average solid angle of 0.004 steradians. For reference, a score of 0.8–0.9 corresponds to a good clustering in this case.

proteins.

t-SNE was able to classify and differentiate all the proteins we tried, from the less complex cases of the monomer/dimer to the higher complex case of sym/asym. Our study shows that the algorithm seems to be able to resolve shape, and atom count to a great extent as well as working with smaller detectors. The most striking is that it could separate the sym and asym structures, which have identical amino acid chains, and very similar structures. These two structure exhibit an IDDT score of 0.89, as seen in Table 1, which is comparable to the level of accuracy that the machine learning folding predictor AlphaFold can predict protein backbone structure [24]. Thus our presented method can distinguish proteins roughly on the same level as AlphaFold can predict structures. This is promising, but we can also conclude that none of the algorithms we used, PCA and t-SNE, were able to separate the proteins if we did not provide the information about the orientation. Protein orientation might be possible to determine either by physically orienting the proteins using external fields [25] or by measuring the trajectories of tag ions in the protein structures, like sulfur [9]. Earlier simulation studies have suggested that adding a thin layer of water around the proteins would both improve the heterogeneity between individual proteins [26–28], and make the explosion footprints more well defined [9] than in this study.

To put the numbers of our results into context we can hypothesize an experiment to see how it compares to our simulations. Utilizing a position-sensitive microchannel plate detector [29] with a 120 mm diameter with a sample-detector distance of 120 mm, which is an achievable sample-detector distance at the SPB/SFX endstation at EuXFEL [30], we

calculate that such detector would cover a solid angle of 0.25π steradians. Compared to the resolution of our simulations, this case corresponds to using only the 10×20 central pixels (see Fig. 4a). Fig. 4b gives an indication of the ARS for any size of detector. We highlight the solid angle value of 0.25π in the Fig. 4b to easily compare a realistic detector geometry to our simulations.

The chances to retrieve structural information from the explosions would most likely improve if one employed more advanced machine learning algorithms than used here. However such algorithms often require training data, which could be complicated to generate experimentally. To achieve high resolution structures from SPI measurements, it would be beneficial to combine the explosion footprints with the diffraction images, and maybe even with an X-ray spectrometer to monitor the atomic processes caused by the ionization in the

sample. Even if the explosion footprints in themselves could not give high resolution structures, they could provide information about global parameters, such as mass and shape of the protein, which possibly can be used as support for phasing algorithms.

This is a simulation study, and what we describe will not be trivial to investigate experimentally. However, based on our findings we believe that efforts towards structural classification of proteins based on Coulomb explosions is an interesting path to improve single particle imaging using XFEL. If coupled with machine learning folding predictors like AlphaFold [24], it could even be a step towards determine the structure based on machine learning and explosion footprints only, without the need of the X-ray diffraction. Protein explosion could in principle be achieved by tabletop femtosecond lasers, which are much more accessible than XFELs.

-
- [1] R. Neutze, R. Wouts, D. Van der Spoel, E. Weckert, and J. Hajdu, Potential for biomolecular imaging with femtosecond x-ray pulses, *Nature* **406**, 752 (2000).
- [2] H. N. Chapman, X-Ray Free-Electron Lasers for the Structure and Dynamics of Macromolecules, *Annual Review of Biochemistry* **88**, 35 (2019), publisher: Annual Reviews Type: Journal Article.
- [3] A. Aquila, A. Barty, C. Bostedt, S. Boutet, G. Carini, D. dePonte, P. Drell, S. Doniach, K. H. Downing, T. Earnest, H. Emlund, V. Elser, M. Gühr, J. Hajdu, J. Hastings, S. P. Hau-Riege, Z. Huang, E. E. Lattman, F. R. N. C. Maia, S. Marchesini, A. Ourmazd, C. Pellegrini, R. Santra, I. Schlichting, C. Schroer, J. C. H. Spence, I. A. Vartanyants, S. Wakatsuki, W. I. Weis, and G. J. Williams, The linac coherent light source single particle imaging road map, *Structural Dynamics* **2**, 041701 (2015).
- [4] C. Caleman, G. Hultdt, F. R. Maia, C. Ortiz, F. G. Parak, J. Hajdu, D. van der Spoel, H. N. Chapman, and N. Timneanu, On the feasibility of nanocrystal imaging using intense and ultra-short x-ray pulses, *ACS nano* **5**, 139 (2011).
- [5] Z. Vager, R. Naaman, and E. P. Kanter, Coulomb Explosion Imaging of Small Molecules, *Science* **244**, 426 (1989), publisher: American Association for the Advancement of Science.
- [6] E. Kukk, K. Motomura, H. Fukuzawa, K. Nagaya, and K. Ueda, Molecular Dynamics of XFEL-Induced Photo-Dissociation, Revealed by Ion-Ion Coincidence Measurements, *Applied Sciences* **7**, 10.3390/app7050531 (2017).
- [7] T. Takanashi, K. Nakamura, E. Kukk, K. Motomura, H. Fukuzawa, K. Nagaya, S.-i. Wada, Y. Kumagai, D. Iablonskyi, Y. Ito, Y. Sakakibara, D. You, T. Nishiyama, K. Asa, Y. Sato, T. Umemoto, K. Kariyazono, K. Ochiai, M. Kanno, K. Yamazaki, K. Kooser, C. Nicolas, C. Miron, T. Asavei, L. Neagu, M. Schöffler, G. Kastirke, X.-J. Liu, A. Rudenko, S. Owada, T. Katayama, T. Togashi, K. Tono, M. Yabashi, H. Kono, and K. Ueda, Ultrafast Coulomb explosion of a diiodomethane molecule induced by an X-ray free-electron laser pulse, *Physical Chemistry Chemical Physics* **19**, 19707 (2017), publisher: The Royal Society of Chemistry.
- [8] R. Boll, J. M. Schäfer, B. Richard, K. Fehre, G. Kastirke, Z. Jurak, M. S. Schöffler, M. M. Abdullah, N. Anders, T. M. Baumann, S. Eckart, B. Erk, A. De Fanis, R. Dörner, S. Grundmann, P. Grychtol, A. Hartung, M. Hofmann, M. Ilchen, L. Inhester, C. Janke, R. Jin, M. Kircher, K. Kubicek, M. Kunitski, X. Li, T. Mazza, S. Meister, N. Melzer, J. Montano, V. Music, G. Nalin, Y. Ovcharenko, C. Passow, A. Pier, N. Rennhack, J. Rist, D. E. Rivas, D. Rolles, I. Schlichting, L. P. H. Schmidt, P. Schmidt, J. Siebert, N. Strenger, D. Trabert, F. Trinter, I. Vela-Perez, R. Wagner, P. Walter, M. Weller, P. Ziolkowski, S.-K. Son, A. Rudenko, M. Meyer, R. Santra, and T. Jahnke, X-ray multiphoton-induced Coulomb explosion images complex single molecules, *Nature Physics* **18**, 423 (2022).
- [9] C. Östlin, N. Timneanu, H. O. Jönsson, T. Ekeberg, A. V. Martin, and C. Caleman, Reproducibility of single protein explosions induced by x-ray lasers, *Physical Chemistry Chemical Physics* **20**, 12381 (2018).
- [10] I. Dawod, S. Cardoch, T. André, E. De Santis, J. E. A. P. Mancuso, C. Caleman, and N. Timneanu, MolDStruct: Modeling the dynamics and structure of matter exposed to ultrafast x-ray lasers with hybrid collisional-radiative/molecular dynamics, *The Journal of Chemical Physics* **160**, 184112 (2024).
- [11] A. Wollter, E. De Santis, T. Ekeberg, E. G. Marklund, and C. Caleman, Enhanced EMC—Advantages of partially known orientations in x-ray single particle imaging, *The Journal of Chemical Physics* **160**, 114108 (2024).
- [12] N.-T. D. Loh and V. Elser, Reconstruction algorithm for single-particle diffraction imaging experiments, *Physical Review E* **80**, 026705 (2009), publisher: American Physical Society.
- [13] V. Mariani, M. Biasini, A. Barbato, and T. Schwede, lddt: a local superposition-free score for comparing protein structures and models using distance difference tests, *Bioinformatics* **29**, 2722 (2013).
- [14] A. M. Waterhouse, G. Studer, X. Robin, S. Bienert, G. Tauriello, and T. Schwede, The structure assessment web server: for proteins, complexes and more, *Nucleic Acids Research* , gkae270 (2024).
- [15] Y. Hirano, K. Takeda, and K. Miki, Charge-density analysis of an iron-sulfur protein at an ultra-high resolution of 0.48 Å, *Nature* **534**, 281 (2016).
- [16] Y. S. Babu, C. E. Bugg, and W. J. Cook, Structure of calmodulin refined at 2.2 Å resolution, *Journal of molecular biology* **204**, 191 (1988).
- [17] J. L. Fallon and F. A. Quijcho, A closed compact structure of native ca²⁺-calmodulin, *Structure* **11**, 1303 (2003).
- [18] R. Golmohammadi, K. Valegård, K. Fridborg, and L. Liljas, The refined structure of bacteriophage ms2 at 2.8 Å resolution,

- Journal of molecular biology **234**, 620 (1993).
- [19] K. Pearson, Liii. on lines and planes of closest fit to systems of points in space, The London, Edinburgh, and Dublin philosophical magazine and journal of science **2**, 559 (1901).
- [20] L. Van der Maaten and G. Hinton, Visualizing data using t-sne., Journal of machine learning research **9** (2008).
- [21] M. N. Brodmerkel, E. De Santis, C. Uetrecht, C. Caleman, and E. G. Marklund, Stability and conformational memory of electrospayed and rehydrated bacteriophage ms2 virus coat proteins, Current Research in Structural Biology **4**, 338 (2022).
- [22] W. M. Rand, Objective criteria for the evaluation of clustering methods, Journal of the American Statistical association **66**, 846 (1971).
- [23] A. Kadek, K. Lorenzen, C. Uetrecht, *et al.*, In a flash of light: X-ray free electron lasers meet native mass spectrometry, Drug Discovery Today: Technologies **39**, 89 (2021).
- [24] J. Jumper, R. Evans, A. Pritzel, T. Green, M. Figurnov, O. Ronneberger, K. Tunyasuvunakool, R. Bates, A. Žídek, A. Potapenko, *et al.*, Highly accurate protein structure prediction with alphafold, Nature **596**, 583 (2021).
- [25] E. G. Marklund, T. Ekeberg, M. Moog, J. L. P. Benesch, and C. Caleman, Controlling protein orientation in vacuum using electric fields, J. Phys. Chem. Lett. **8**, 4540 (2017).
- [26] A. Patriksson, E. Marklund, and D. van der Spoel, Protein structures under electrospray conditions, Biochemistry **46**, 933 (2007).
- [27] J. E. M. Stránský, Z. Jurek, C. Fortmann-Grote, L. Juha, R. Santra, B. Ziaja, and A. Mancuso, Effects of radiation damage and inelastic scattering on single-particle imaging of hydrated proteins with an x-ray free-electron laser, Scientific Reports **11** (2021).
- [28] T. Mandl, C. Östlin, I. E. Dawod, M. N. Brodmerkel, E. G. Marklund, A. V. Martin, N. Timneanu, and C. Caleman, Structural heterogeneity in single particle imaging using x-ray lasers, The Journal of Physical Chemistry Letters **11**, 6077 (2020), pMID: 32578996, <https://doi.org/10.1021/acs.jpcclett.0c01144>.
- [29] Z. Korkulu, L. Stuhl, S. Naimi, Z. Dombrádi, K. Hahn, J. Moon, D. Ahn, Z. Halász, and G. Hudson-Chang, A position-sensitive large-area microchannel plate detector with digital data-acquisition system for studies of exotic nuclei, Nuclear Instruments and Methods in Physics Research Section B: Beam Interactions with Materials and Atoms **541**, 232 (2023).
- [30] A. P. Mancuso, A. Aquila, L. Batchelor, R. J. Bean, J. Bielecki, G. Borchers, K. Doerner, K. Giewekemeyer, R. Graceffa, O. D. Kelsey, *et al.*, The single particles, clusters and biomolecules and serial femtosecond crystallography instrument of the european xfel: Initial installation, Journal of synchrotron radiation **26**, 660 (2019).